

The rat orbital and agranular insular prefrontal cortical areas: a cytoarchitectonic and chemoarchitectonic study

Henri J. J. M. Van De Werd · Harry B. M. Uylings

Received: 15 August 2007 / Accepted: 30 November 2007 / Published online: 9 January 2008
© Springer-Verlag 2007

Abstract Cytoarchitectonic characterization of borders is necessary for stereological studies (e.g., total cell number estimation), in which particular cortical areas have to be defined. In this study, cytoarchitectonic characteristics are described and illustrated for the rat ventral or orbital frontal cortical areas, i.e., the lateral-, ventrolateral-, ventral- and medial-orbital areas; and for the lateral frontal cortical areas, i.e., the agranular insular and the dorsolateral orbital cortical area. Each cytoarchitectonic-defined boundary is corroborated by one or more of the immunocytochemical stainings for dopaminergic fibers, SMI-32 positive neurons, calbindin and parvalbumin positive neurons. Each immunocytochemical staining, however, shows a characteristic subset of the cytoarchitectonic borders. The dorsal agranular insular area (AId) and the dorsolateral orbital area (DLO) have been subdivided into a dorsal and a ventral part based upon differences between these parts in the Nissl and immunocytochemical stainings. The posterior part of VLO has a different structure and is, therefore, indicated as VLOp (VLO, posterior part).

Keywords Cortical parcellation · Infralimbic · Prelimbic · Medial orbital · Ventrolateral orbital and lateral orbital cortical areas · Claustrum · SMI-32 · Dopamine · Calbindin and parvalbumin

Abbreviations

AId ₁	Dorsal agranular insular area, dorsal part
AId ₂	Dorsal agranular insular area, ventral part
AIV	Ventral agranular insular area
AIP	Posterior agranular insular area
CB	Calbindin
cc	Corpus callosum
CL	Claustrum
DA	Dopamine
DI	Dysgranular insular area
DLO ₁	Dorso-lateral orbital area, dorsal part
DLO ₂	Dorso-lateral orbital area, ventral part
Fr2	Frontal area 2
FPI	Lateral frontal polar area
FPm	Medial frontal polar area
G	Granular cortex
GI	Granular insular cortex
IL	Infralimbic area
LO	Lateral orbital area
MO	Medial orbital area
OB	Olfactory bulb
PFC	Prefrontal cortex
PL	Prelimbic area
PV	Parvalbumin
VLO	Ventrolateral orbital area
VLOp	Ventrolateral orbital area, posterior part
VO	Ventral orbital area

H. J. J. M. Van De Werd · H. B. M. Uylings (✉)
Department of Anatomy and Neuroscience,
VU University Medical Center,
Graduate School Neuroscience Amsterdam,
P. O. Box 7057, 1007 MB Amsterdam, The Netherlands
e-mail: hbm.uylings@vumc.nl

H. B. M. Uylings
Department of Psychiatry and Neuropsychology,
Division Brain and Cognition, School for Mental Health
and Neuroscience, University of Maastricht,
European Graduate School of Neuroscience (EURON),
Maastricht, The Netherlands

Introduction

Several studies have studied the medial and lateral prefrontal cortical subareas of the rat in detail (Krettek and Price 1977; Van Eden and Uylings 1985; Uylings and Van Eden 1990; Ray and Price 1992). Krettek and Price (1977) described the ventral/orbital subareas of rat PFC. These orbital areas were mainly defined on the basis of thalamic connections (Krettek and Price 1977; Ray and Price 1992; Reep et al. 1996). A further study to characterize the cytoarchitectonic features of the borders between these ventral/orbital subareas is of importance for stereological studies on total number of neurons and/or glia cells in these areas, examined in Nissl stainings (Rajkowska et al. 2005) and to determine if the different cytoarchitectonic areas correspond with the differential pattern of connectivity with other cortical, striatal and thalamic regions (Uylings et al. 2003; Groenewegen and Witter 2004; Gabbott et al. 2005; Hoover and Vertes 2007). The latter, also because of the present questions whether or not a particular part of the orbital cortex (i.e., the ventrolateral orbital cortex) belongs to the prefrontal cortex (Ray and Price 1992; Reep et al. 1996; Uylings et al. 2003). The cytoarchitectonic delineation of rat orbital prefrontal areas needs to be based on criteria consistently visible in microscopic cell stainings of different rat brains. The purpose of this study is to provide these consistent features to distinguish the boundaries of the different sub areas of the rat orbital and agranular insular prefrontal cortex. In addition, we compared the location of cytoarchitectonically-defined borders with boundaries visible in immunocytochemical stainings for dopaminergic fibers, SMI-32, parvalbumin and calbindin positive neurons. The distribution of dopaminergic fibers is different across the cortical subareas, whereas the distribution of the noradrenergic and serotonergic fibers is more homogeneous (Uylings et al. 2003 and unpublished observations). The nonphosphorylated neurofilament protein stained with the monoclonal SMI-32 antibody has been applied to differentiate between cortical areas and stains a particular subpopulation of pyramidal neurons (e.g., Hof and Morrison 1995). In addition, the apical dendrite orientation of these cells is visible in SMI-32 staining and thereby the orientation of several areal boundaries. The calcium binding protein staining with parvalbumin and calbindin stain different subpopulations of nonpyramidal neurons and have been used also for strengthening of some cortical boundaries (e.g., Paxinos et al. 1999). In the literature, such a combined cytoarchitectonic and immunochemoarchitectonic study of the rat orbital and agranular insular cortex is lacking.

Materials and methods

The studies were approved by the local Animal Experimentation Committee and were carried out in agreement with Dutch animal acts and the European regulations (Guideline 86/609/EEC).

The cytoarchitectonic study is based on the examination of 11 adult male Wistar rats (Harlan/CPB, Horst, The Netherlands) weighing about 275–400 g. The animals were socially housed in groups of four in standard type IV Macrolon cages and kept under a day/light cycle (white light from 7 AM till 7 PM, dimmed red light from 7 PM till 7 AM. Food and water were available ad libitum. Before perfusion, the animals were under deep pentobarbital anesthesia (1 ml/kg body weight, i.p.). The animals were perfused with a 4% formaldehyde solution in saline and subsequently fixed in skull for 24 h, and postfixed for another 24 h. From a large part of the animals (i.e., $n = 8$), the brains were immersion fixed in a 4% formaldehyde solution in saline after a postmortem delay of 0 h. These brains form a part of a postmortem delay effect study. In these immersion-fixed brains, spots with pyknotic reaction were not incorporated in our study when they were present. The brains of these 11 rats were embedded in celloidin and sectioned coronally at 50 μm . These sections were serially collected in 70% alcohol solution (Kamstra and Uylings 1983) and after rinsing in distilled water for about 5 min, they were Nissl stained in cresylviolet solution (200 ml distilled water, 1 g cresylviolet, 2 ml acetic acid) for about 2 min, sometimes 6–7 min.

Brains of 15 additional adult male Wistar rats (weighing 275–400 g) have been immunocytochemically stained. From three brains, consecutive sections of each brain have been stained with different antibodies among which were SMI-32, parvalbumin, and calbindin, and Nissl. In order to obtain series with a smaller interval than in the last-mentioned three brains, two brains have been used for each of the immunocytochemical stainings (except for DA) and some consecutive sections with Nissl staining. Thus a total of five brains have been prepared for each of SMI-32, PV and CB immunocytochemical stainings. Six animals have been used for DA staining. No Nissl staining was prepared from these DA brains. The immunocytochemical stainings were obtained with dopamine (DA) antibody (Geffard et al. 1984), SMI-32 antibody (Sternberger Monoclonals Inc., Baltimore, Md, USA: monoclonal antibody to non-phosphorylated neurofilaments, Lot Number: 11; presently distributed through Covance Research Products, Berkeley, Ca, USA), monoclonal anti-calbindin D-28K antibody (Sigma, St Louis, Mo, USA: Product Number: C-9848, Clone Number: CB-955, Lot Number: 015K4826), and monoclonal anti-parvalbumin antibody (Sigma, St Louis,

Mo, USA: Product Number: P-3171, Clone Number: PA-235, Lot Number: 026H4824).

Rats to be stained for DA were intracardially perfused, under deep pentobarbital anesthesia (1 ml/kg body weight, i.p.), with saline followed by fixative. For DA staining, the fixative was 5% glutaraldehyde in 0.05 M acetate buffer at pH 4.0. After perfusion the brains were removed from the skull and postfixed for 30 min. Then the brains were immersed in 0.05 M Tris containing 1% Sodium disulfite ($\text{Na}_2\text{S}_2\text{O}_5$) at pH 7.2 (De Brabander et al. 1992). Rat prefrontal cortex was sectioned coronally at 50 μm by a vibratome. These sections were stained overnight in a cold room at 4°C using the polyclonal primary antibody sensitive for DA raised in the Netherlands Institute for Brain Research (NIBR), Amsterdam (Geffard et al. 1984) of which the specificity has been demonstrated previously (Kalsbeek et al. 1990). DA antiserum was diluted 1:2,000 in 0.05 M Tris containing 1% $\text{Na}_2\text{S}_2\text{O}_5$ and 0.5% Triton X-100, pH 7.2. After overnight incubation, the sections were three times washed with Tris buffered saline (TBS, 3 \times 10 min) and subsequently incubated in the secondary antibody goat-antirabbit, also raised at NIBR, at 1:100 for 1 h. and, after rinsing 3 \times in TBS, incubated in the tertiary antibody, peroxidase-anti-peroxidase, at 1:1,000 for 60 min. Both the secondary and the tertiary antibodies were diluted in TBS with 0.5% gelatin and 0.5% Triton X-100. For visualization, the sections were transferred into 0.05% diaminobenzidine (DAB; Sigma) with 0.5% nickel ammonium sulphate. The reaction was stopped after a few minutes by transferring the sections to TBS (3 \times 10 min), then the sections were mounted on slides, air dried, washed, dehydrated and mounted.

Rats to be stained with antiparvalbumin, anticalbindin and SMI-32 were fixed with 4% formaldehyde solution in 0.1 M phosphate buffer at pH 7.6. Rat prefrontal cortex was sectioned coronally at 50 μm by a vibratome. To prevent endogenous peroxidase activity, free-floating sections were pretreated for 30 min in a Tris-buffered saline (TBS) solution containing 3% hydrogen peroxide and 0.2% Triton X-100. To prevent nonspecific antibody staining, these sections were placed in a milk solution (TBS containing 5% nonfat dry milk and 0.2% Triton X-100) for 1 h. Incubation of the primary antibody, directly after the milk step, was carried out overnight in a cold room at 4°C. The primary antibodies were diluted in above-mentioned milk solution: SMI-32 at 1:1,000, parvalbumin antibody at 1: 1,000, and calbindin antibody at 1: 250. For the monoclonal SMI-32, parvalbumin and calbindin antibodies, raised in mice, we used peroxidase-conjugated rabbit antimouse (1:100 in 5% milk solution with 0.2% Triton X-100) as secondary antibody. Visualization took place in 0.05% diaminobenzidine enhanced with 0.2% nickel ammonium sulphate. The reaction was stopped after a

few minutes by transferring these sections to TBS (3 \times 10 min), then the sections were rinsed in distilled water (3 \times 10 min), mounted on slides, air dried, washed, dehydrated and mounted.

Control sections incubated according to the same procedure described above, but omitting the primary antibody were all negative.

All sections have been cut coronally, because the coronal plane offers in general the best view to differentiate between the subareas of the prefrontal cortex.

In general, a Zeiss Standard WL microscope with a 63 \times magnification (plan objective 6.3 \times) has been used. For a complete overview, a 25 \times magnification and for more details a 100 \times magnification (plan objective 10 \times) has been used, respectively. For the illustrations, tiled images were digitized using the Zeiss Axioskop 40 with a plan 10 \times objective and Image Pro Plus software package. These digital tiff images were cropped and minimally contrasted with Adobe Photoshop 7.0 program. The curved boundaries and letter setting were prepared for the illustrations by means of CorelDraw 9 software. The nomenclature for the subareas of the prefrontal cortex is mainly based on the descriptions of Krettek and Price (1977), Uylings and Van Eden (1990), Ray and Price (1992), and see Uylings et al. 2003.

Results

Figure 1 shows the schematic view of the medial, lateral and orbital regions of the prefrontal cortex (PFC) of the rat. The position of the Nissl-stained sections, which display the orbital and the agranular insular cortical areas in Fig. 2, is indicated by the vertical lines above the medial view of the PFC. These cortical subareas have been identified in all Nissl-stained brains. No left–right differences were noted in the characteristics of these subareas. The characteristic features of the borders between these areas are specified below.

The dysgranular insular (DI) and the granular insular (GI) cortex

The dysgranular insular cortex (DI), shown in Fig. 3, is located dorsally to the agranular insular (AI) prefrontal cortex. The most important characteristics of its border on the granular insular cortex (GI) are seen in layers II, III, IV and in the outer sublayer of layer V. In GI, layer IV is very well distinguishable as a dark band of closely packed granular cells flanked on its inner side by the light outer sublayer of layer V and on its outer side by the homogeneous layers II–III. In GI, the width of layers II, III and IV,

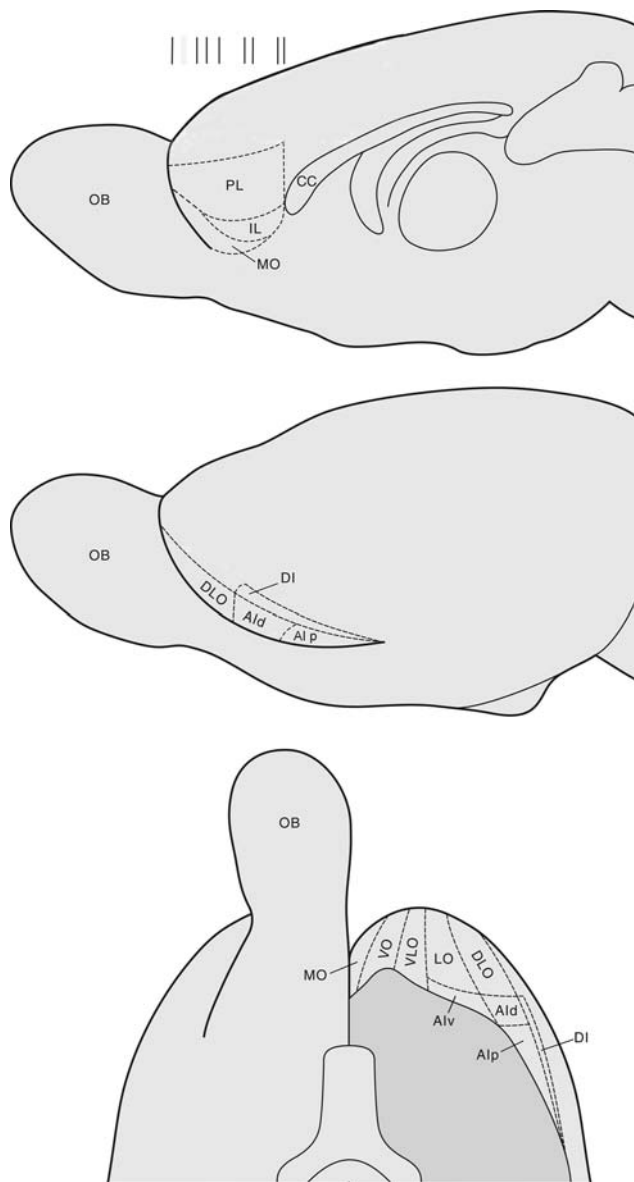


Fig. 1 Schematic view of the medial, lateral and ventral areas in the frontal lobe of the rat brain. The lines above the medial view indicate the levels in the frontal lobe of the eight Nissl-stained sections shown in Fig. 2. The ventral view (*lowest panel*) shows both hemispheres; the olfactory bulb (*OB*) and olfactory tract have been removed from beneath the left hemisphere to display the ventral orbital and insular cortical areas

taken together, tends to become less when the border on DI is approached. In DI, layers III, IV and the outer sublayer of layer V are homogeneous, sometimes including layer II.

In the SMI-32 staining shown in Fig. 4b, the granular insular cortex is heavily stained in layers III, V and VI, but near the agranular insular area this heavy staining disappears; first in layer III and then also in layers V and VI. In the sections stained with parvalbumin antibody shown in Fig. 4d, DI is not clearly visible. DI appears in the parvalbumin staining as a small transition zone between the

heavily stained layers of GI and the much less stained layers of AId. This is especially apparent in the background staining of layers II and III. In the calbindin antibody stained sections (Fig. 4e), DI is not recognizable as a distinct area. Also in the dopamine antibody staining (Fig. 4c), neither DI can be distinguished as the granular cortex, or the dysgranular insular cortex, nor the dorsal part of AI is stained by dopamine except for the layer VIb.

The dysgranular insular (DI) and the dorsal agranular insular (AId) area

In Nissl-stained sections ((Figs. 3, 4a), the larger cells of layer V shift in AId to a more superficial position than in DI. This coincides with the complete disappearance of layer IV and with a change in layer II. In AId, layer II is characterized by a rather homogeneous densely packed dark band, which is sharply divided from a sparsely packed layer III. Sometimes, however, there is not such a clear sudden shift in layer V. Then the other changes occurring in layer V will help to define the border, such as the characteristic vertical rows of somata of layer V, arranged closely to each other in AId, in contrast to the situation in the granular and dysgranular insular cortex, where layer V is less columnarly organized.

A typical feature in the transition of GI via DI to AId is the shift of the most superficial interlaminar cell-sparse zone in GI, i.e. superficial sublayer of layer V, to the more superficial interlaminar lying cell-sparse zone in AId, i.e. layer III (Figs. 3, 4a).

In the SMI 32-staining (Fig. 4b), the well-stained layers III, V and VI in GI and DI disappear at the border upon AId. AI is not stained by SMI-32 antibody, except perhaps for very faint staining of layer VI. In the parvalbumin-stained sections (Fig. 4d), layers II, III, and IV have a dark background in the area dorsal to AId, while in AId, layers II–III are paler. In the calbindin-stained sections (Fig. 4e), the border between DI–GI and AId is difficult to distinguish. However, more neurons are distinct in the layers III–VI in AI than those in DI–GI. In the dopamine antibody staining (Fig. 4c), no border between DI and AId is visible.

Rostral to AId: dorsal lateral orbital area (DLO)
borders granular cortex (G)

In the Nissl stained section shown in Figs. 5a and 6e, layers II, III and IV dorsal to DLO are rather homogeneous whereas in DLO layers II, III and V are more distinguishable from each other. Layer II in DLO is broader than the layer II in the granular cortex. The cells of layer V are larger in the granular cortex than in DLO. Moreover the

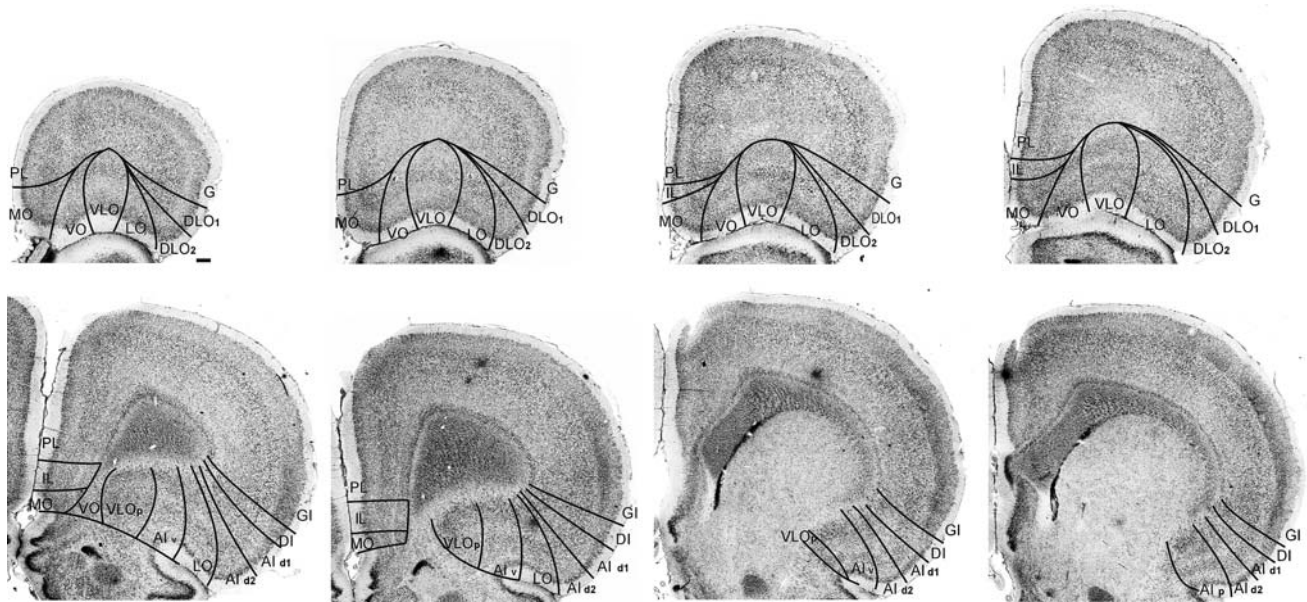


Fig. 2 Overview of orbital and lateral prefrontal subareas in Nissl-stained coronal sections at eight different levels in anterior–posterior direction as specified in Fig. 1

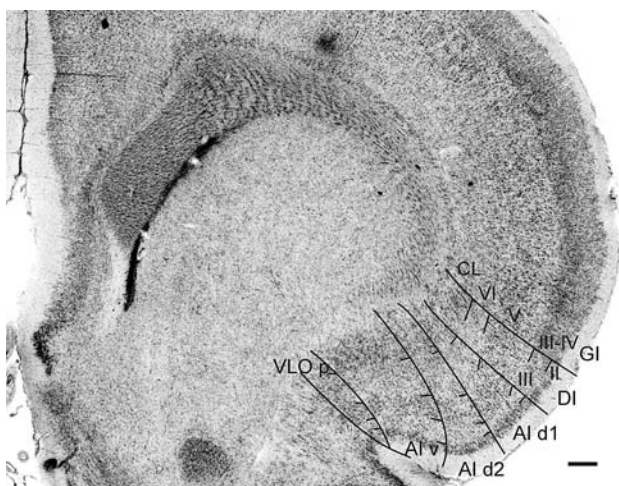


Fig. 3 The Nissl-stained section (a magnification of the seventh panel in Fig. 2) shows the features of the granular insular area (*GI*), the dysgranular insular area (*DI*), the two subareas of the dorsal agranular insular area (*Aid₁* and *Aid₂*), the ventral agranular insular area (*Aiv*) and the posterior area of ventrolateral orbital cortex (*VLOp*). Scale bar 150 μ m

cells of layer V are more clearly arranged in vertical rows in DLO than in the granular cortex (Fig. 5a).

In the SMI-32 staining (Figs. 5b, 6a), the border between the granular cortex and DLO is marked by the disappearance of the dark layer III of the granular cortex. In the parvalbumin staining (Fig. 6d), the background staining of layers II and III in G is stronger than those in DLO. This holds for a lesser extent also in layer V. In the calbindin staining (Fig. 6b), the border between DLO and the granular cortex cannot be distinguished easily although

the layers II–III are more homogeneous in the granular cortex than in DLO.

In the dopamine staining (Fig. 6c), no border is visible between DLO and the granular cortex. The border drawn in this Fig. 6c has been extrapolated from the border observed in the Nissl staining and other immunocytochemical stainings.

Dorsolateral orbital (DLO) area compared to the dorsal agranular insular area (Aid)

The agranular DLO lies anterior to Aid. The claustrum is generally absent underneath DLO, whereas underneath Aid, the claustrum is present. The cytoarchitectonic transition of DLO into Aid at the posterior border of DLO is rather gradual. The dorsal border of the agranular dorsolateral orbital area (DLO) is on the granular cortex (Fig. 7), whereas the dorsal border of Aid is on the dysgranular insular cortex. Dorsally to DLO, the layer IV cells in the granular cortex are more difficult to discern than they are in the granular cortex dorsally to DI and Aid. The shift of the large cells in layer V visible at the dorsal border of DLO is generally less impressive than the one at the border between DI and Aid (Figs. 7, 3). DLO is also characterized by a rather homogeneous and dark layer II, which is relatively wider and generally less sharply distinct from layer III (Figs. 6e, 7) than it is in Aid (Fig. 3).

The SMI-32 staining layers V and VI in DLO are generally more intensely stained than they are in Aid, except for the most anterior part of the frontal lobe

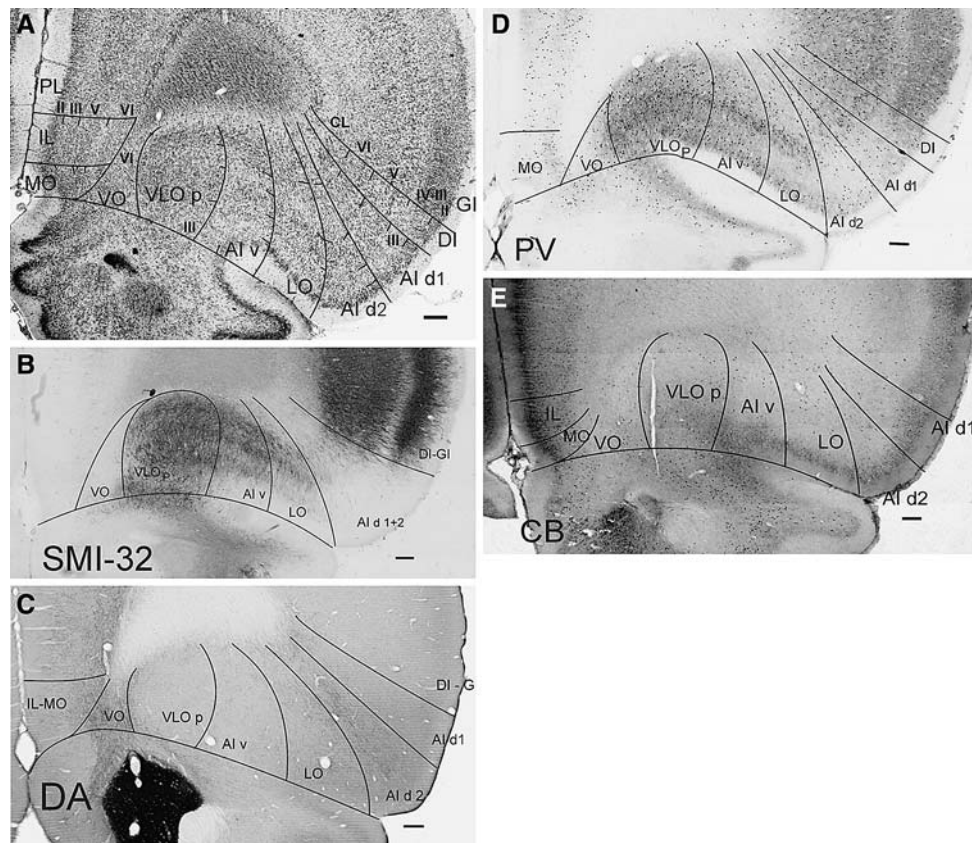


Fig. 4 **a** The coronal Nissl-stained section (a magnification of the fifth panel in Fig. 2) illustrates the border between *GI* and *DI* and the difference in layer II between *Aid₁* and *Aid₂*. *LO* shows its typical clustered layer II. In *Alv*, the sublayers of layer V are less densely packed than those in *LO*. In *VLOp*, homogeneity of layers III, V and VI with the claustrum is characteristic. **b** *SMI-32* stained section displaying the cross-section through *VO*, *VLOp*, *Alv*, *LO*, *Aid₁* and *Aid₂*, and *DI* and *GI*. **c** Dopamine staining showing the subdivision

between *Aid₁* and *Aid₂* due to the much higher density of the dopaminergic fibers in *Aid₂*. Many dopaminergic fibers run through the connection of caudal part of *VO* and the retrolubar region. **d** The parvalbumin staining in *VLOp* is rather homogeneous. **e** Calbindin stained section showing the difference between *Aid₁* and *Aid₂* visible in layer II. *LO* shows a dark, narrow layer II. The boundaries between the cortical subareas have been extrapolated from the nearest consecutive Nissl-stained section. Scale bars 150 μ m

(Compare Figs. 5b, 6a and 4b). In the parvalbumin staining, the staining of layers V and VI is stronger in *DLO* than in *Aid* (Compare Figs. 6d and 4d). In the calbindin staining (Figs. 6b, 4e), the differences between *DLO* and *Aid* are relatively small. In the dopamine antibody staining no difference is visible between *DLO* and *Aid*.

Two subareas in the dorsal agranular insular (*Aid*) and the dorsolateral orbital (*DLO*) area

In Nissl-stained sections, the dorsal agranular insular cortex (*Aid*), Figs. 3 and 4a, as well as the dorso-lateral orbital area (*DLO*), Fig. 7, can generally be subdivided in a dorsal and a ventral part which we propose to call *Aid₁* and *Aid₂*, or *DLO₁* and *DLO₂*, respectively, of which part 1 is dorsal to part 2. The following features distinguish these subareas. In *Aid₁* and *DLO₁*, layer II is rather homogeneous, but in *Aid₂* and in *DLO₂*, layer II

is less equally packed except for cells bordering layer I. The rows of cells in layer V are closer to each other in *Aid₂* and *DLO₂* than in *Aid₁* and *DLO₁* (Figs. 3, 4a for *Aid* and Fig. 7 for *DLO*). In *DLO* as well as in *Aid*, layer II becomes less wide in the dorsoventral direction.

This subdivision in *Aid* and *DLO* seen in the Nissl-stained sections, can also be recognized in some immunocytochemically stainings, especially the dopamine staining. In the dopamine staining (Figs. 4c, 6c), a clear difference is visible between *DLO₁* and *DLO₂*, and between *Aid₁* and *Aid₂* due to a high dense staining of dopaminergic fibers in *DLO₂* and *Aid₂*, respectively, in contrast to *DLO₁* and *Aid₁*. In the calbindin-stained sections, the cells of layer II are more heterogeneously distributed in *DLO₂* than in *DLO₁* (Fig. 6b), just as in the Nissl-stained sections. This difference is also visible in the calbindin staining of *Aid₁* and *Aid₂*. In the parvalbumin-staining, no consistent difference is visible, although it is

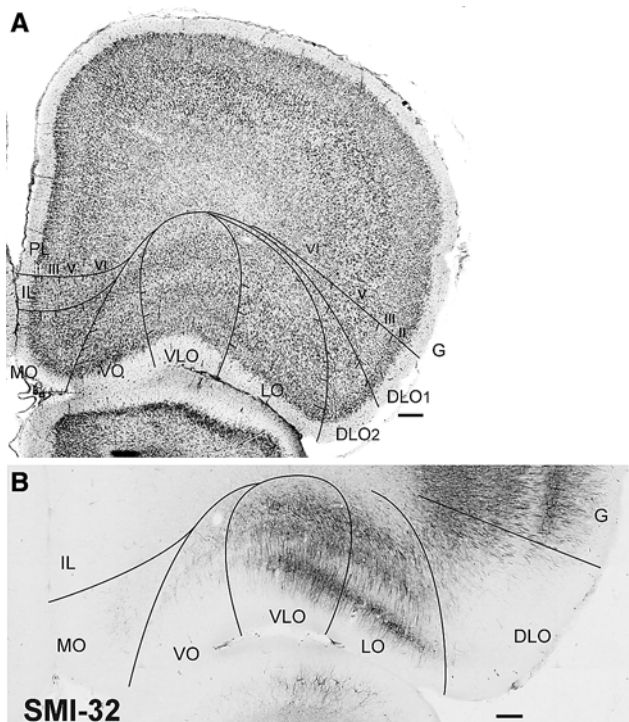


Fig. 5 **a** The Nissl staining (a magnification of the fourth panel in Fig. 2) illustrates the difference between *DLO*₂ and *LO*, especially in layers III and V and the features of *VLO*. *VLO* has a more distinct layering pattern than *VLO*_p (cf. Fig. 4a). The layer II cells in *MO* are smaller than those in *VO*. **b** No *SMI-32* staining is visible in layers II and III of *DLO*, but there is staining in layers V and VI. In *LO*, a clear zone is present between the layers III and V, whereas they are more “connected” in *VLO*. The *SMI-32* staining is denser in layer III, and the stained layers are more differentiated in *VLO* than in *VLO*_p (cf. Fig. 4b). Scale bars 150 μm

sometimes possible to divide the areas *AId* and *DLO* in a dorsal and a ventral part on the basis of a difference of staining in layers V and VI (Figs. 4d, 6d). In the *SMI-32* stained sections (Figs. 4b, 6a), *DLO* and *AId*, except for their deepest layers, are not stained at all so a subdivision between *DLO*₁ and *DLO*₂ or between *AId*₁ and *AId*₂ cannot be made in this staining.

The posterior agranular insular (*AIp*) area

On basis of tracing studies (e.g., Groenewegen 1988; Uylings and Van Eden 1990), the caudal part of the agranular insular cortex, called the posterior agranular insular cortex (*AIp*), is considered not to belong to the prefrontal cortex (Figs. 2, 8b). Figure 8b shows that *AIp* is cytoarchitectonically characterized with a marked separation of all sublayers by cell-sparse zones [i.e., 8–9 (sub) layers] and also by the small cells of its layer V. *AIp* borders dorsal to *DI* (Van Eden and Uylings 1985) with the exception of the

most anterior part of *AIp*, where it borders dorsally to *AId* (Fig. 8b).

In the *SMI*-stained section (Fig. 9c), *AIp* is not stained or is stained only very faintly in layer VI, just like *AId*, but the underlying claustrum shows *SMI*-positive staining. The granular insular cortex has intensely stained layers III and V. The border between *AIp* and *DI* coincides with the disappearance of *SMI*-positive staining in both the layers III and V. In the parvalbumin staining (Fig. 9b), the dorsal border of *AIp* coincides with the disappearance of dark background staining of layer III in *DI*–*G*. In the calbindin staining (Fig. 9a), *AIp* is characterized by its densely stained layers II and V. The (background) staining in layer V in *AIp* is not well visible in the calbindin staining of *AId*.

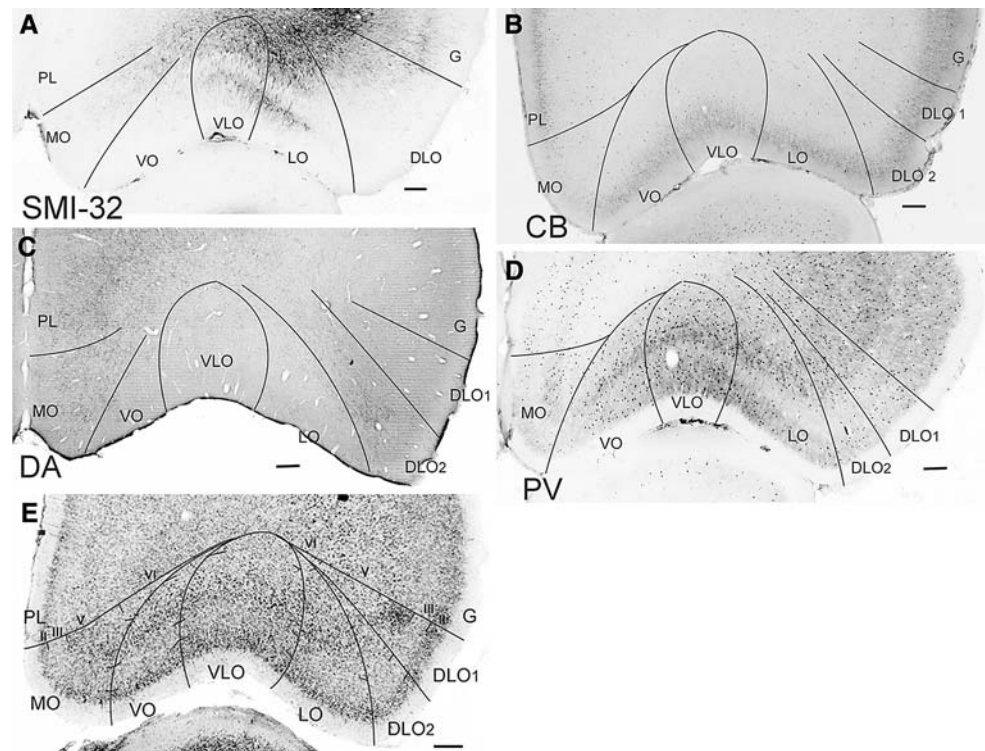
In the dopamine staining (Fig. 9d), *AIp* is well stained, but *DI* and *GI*, and large part of claustrum lack dopamine staining.

The dorsolateral orbital (*DLO*) and the lateral orbital (*LO*) areas

In Nissl-stained sections (Fig. 5a), the border between the dorso-lateral orbital area and the lateral orbital area (*LO*) is characterized by changes in the layers II, III and V. Layer II is plain and dark in the dorso-lateral orbital area, but clustered and often narrower than layer II in the lateral orbital area. The cells of layer II are larger and rounder in the lateral orbital area than in *DLO*. The cells of layer III are generally more densely packed, but in a narrower band, in *LO* than in *DLO* (Fig. 5a). Sublayers in layer V are often visible in the lateral orbital area and less in the dorso-lateral orbital area. Moreover the pyramidal cells of layer V in *DLO* are arranged in vertical rows consisting of many cells, whereas in the lateral orbital area they are packed in a much less broad layer. Rostrally, the rows in layer V of *DLO* are less distinguishable due to the cutting plane. The *DLO/LO* border is mostly found just medially to the ventrolateral crown of the frontal lobe (Fig. 5a).

In the dopamine staining (Fig. 6c), the border is very clear, since dopaminergic fibers of layers V and VI of the ventral part of *DLO* (*DLO*₂) are well visible, but in *LO* the dopamine staining is nearly absent. In the *SMI 32*-stained sections (Figs. 5b, 6a), layers III, V and VI in *LO* are well stained, except of the most lateral part of layer III in *LO*, while in *DLO* layer V and VI are less and layers II and III are not stained. Thus the border between *LO* and *DLO* is not well visible in *SMI-32*. In the parvalbumin staining (Fig. 6d), layer V in *DLO*₂ and the background in layer II and III and in V and VI is less stained than in *LO*. The border according to the parvalbumin stain parallels the border between *DLO* and *LO* in the Nissl-stained sections (Fig. 6). The calbindin staining (Fig. 6b) and especially the

Fig. 6 **a** No SMI stained cells are present in the upper layers of area *DLO* and the lateral part of *LO*. A stained layer III is visible in the medial part of *LO*. **b** The most conspicuous feature in this calbindin stained section is the sparse staining in *MO*. **c** In *DLO*₂, and *MO*, dopaminergic fibers are visible in all layers. The other orbital areas contain very few fibers. **d** The parvalbumin staining shows a more clear layering in *VLO* than in *VLOp* (cf. Fig. 4d). The superficial layers in *VO* layer II are less stained than in *VLO*. **e** Nissl-stained section (rostral to the second panel level in Fig. 2) illustrating differences between *PL*, *MO*, *VO*, *VLO*, *LO*, and *DLO*₁ and *DLO*₂. Scale bars 150 μm



dopamine staining (Fig. 6c) show also a border just medial to the ventrolateral gyral crown of the frontal lobe.

The dorsal agranular insular area (AId) and the lateral orbital area (LO)

The cytoarchitectonic characteristics of *DLO* are changing to that of AId before *LO* changes into AIV (Fig. 4). Therefore, the anterior part of AId borders on *LO* and more posteriorly on AIV. The dark layer II of AId with its sharp border on layer III changes in *LO* into a dark clustered layer that has a less sharp border on layer III (Figs. 4a, 8a). The cells of layer III of *LO* are more densely packed in a narrower band in contrast to the homogeneous layer III of AId. The cells of layer V are more densely packed and not arranged in vertical rows in *LO* while they are arranged in vertical rows in AId (Fig. 4a).

In the SMI-32 staining (Fig. 4b), the AId/*LO* border is indicated by layers V and VI, which are more stained in *LO* than in AId. In the parvalbumin staining (Fig. 4d), layer V in *LO* is darker with more densely packed cells than in AId. In both the SMI-32 and the parvalbumin staining, the border between *LO* and AId₂ is better discernible than between *LO* and *DLO*₂ in the lower layers (Figs. 4b, d, 5b, 6a, d, respectively). In the calbindin staining (Fig. 4e), layer II of AId is broader than layer II in *LO*, which is clustered and narrow. In the dopamine staining (Fig. 4c), AId is heavily stained whereas *LO* is only slightly stained.

The dorsal agranular insular (AId) and the ventral agranular insular (AIV) area

The ventral agranular insular area lies posterior to *LO*. In Nissl staining (Fig. 3), the border between the dorsal agranular insular area and the ventral agranular insular area is characterized by layer II being plain and dark in the dorsal agranular insular area (AId), and equally dark, but more clustered in the ventral agranular insular (AIV) area. The cells of layer III are less densely packed in the ventral agranular insular area than in the dorsal agranular insular area. In AIV, layer V is more distinct from layer VI than in AId. The last mentioned characteristic is an important indication of AIV.

In the SMI-32 staining (Fig. 4b), layers III, V and VI are well stained in AIV while in AId the staining of its layers is nearly absent. Although in Fig. 4, AId does not border directly AIV, the differences between the well-stained AIV and the barely stained AId make it easy to assess the border between AId and AIV in sections where they have a common border. In the parvalbumin-stained sections (Fig. 4d), the layers II, III and V in AIV are more stained than in AId. As for the SMI-32, staining was mentioned but we did not include in this study a picture of the direct border between AId and AIV, since the differences between AIV and AId are also obvious in Fig. 4d. In the calbindin antibody staining (Fig. 4e), the border between AId and AIV is mainly distinguished by the following feature. In AId, layer II is dark and densely packed with cells, while in AIV the

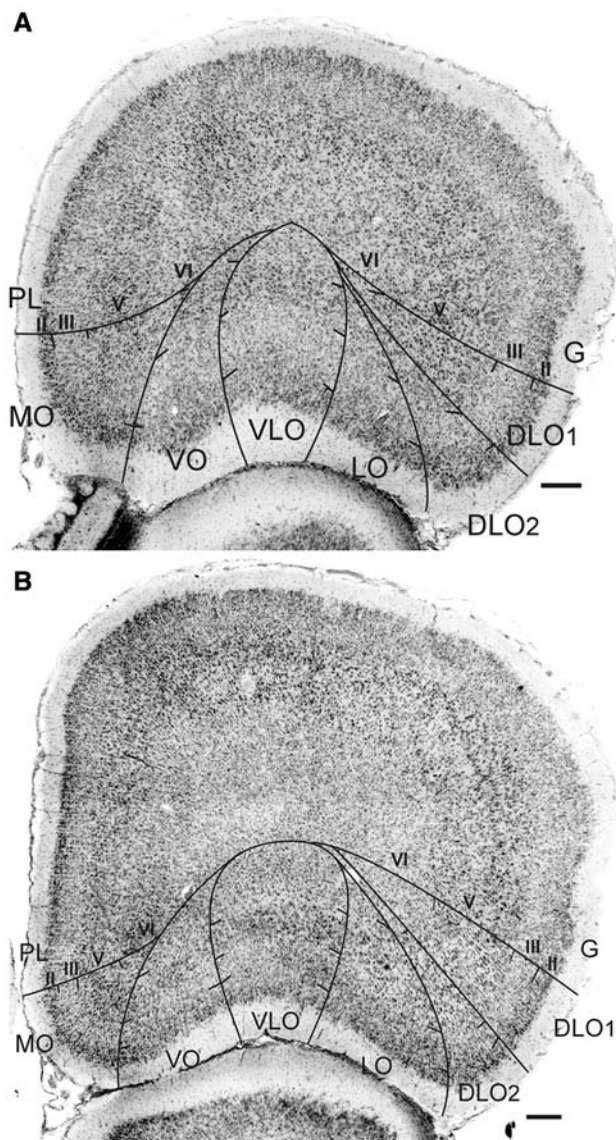


Fig. 7 Nissl-stained sections illustrating the subdivision of *DLO*. The lateral part of layer II of *LO* is more clustered than the medial part. In *VLO*, layers II and III are homogeneous and their somata appear in vertical rows. Layer II in *MO* shows a dispersed band of cells, which are distinct from layers I and III. **a** At the rostral pole level of first panel in Fig. 2b and at the level of the third panel in Fig. 2. Scale bars 150 μ m

positive cells in layer II are wider spread. In the dopamine-stained sections (Fig. 4c), the layers II, III, V and VI in *AId₂* are intensely stained, whereas in *AIv*, the staining is nearly absent, resembling the *AId₂/LO* border in Fig. 4c.

The lateral orbital (LO) and the ventral agranular insular (*AIv*) area

LO lies anterior to the ventral agranular insular area (*AIv*), Figs. 1 and 2. In Nissl-stained sections shown in Figs. 4, 8a

and 10, the lateral orbital area (*LO*) and the ventral agranular insular area (*AIv*) are distinguishable by the following features. The cells in layer III of *LO* are densely packed, often in a narrow band, while they are less densely packed and more homogeneously spread in *AIv*. The outer and inner sublayers of layer V are better visible in *AIv* than in *LO*. Viewing these characteristics, the anterior part of *AIv* can be found in some coronal sections to be positioned between the lateral orbital area and the ventrolateral area (*VLO* and *VLO_p*), Figs. 4a, 8a, and 10. In the SMI-32 staining (Fig. 4b), the border between *AIv* and *LO* coincides with the transition between the stronger staining in layers III, V and VI in *AIv* and the lesser staining in *LO*. In the parvalbumin staining (Fig. 4d), the general background staining is heavier in *AIv* than in *LO* and also the cells in layer V are more densely packed in *AIv* than in *LO*. In the calbindin staining (Figs. 4e), a definite border between *AIv* and *LO* is not well visible, but a transition of the clustering in layer II in *LO* into the more homogeneous layer II in *AIv* (Fig. 4e) does agree with the border between *LO* and *AIv* in the Nissl-stained sections. In the dopamine staining (Fig. 4c), the border between *AIv* and *LO* can only be extrapolated from Nissl staining, since the difference in staining is too faint.

The lateral orbital (*LO*) and the ventrolateral orbital (*VLO*) area

In Nissl-stained sections shown in Fig. 5a and 7, the border between the lateral orbital area and the ventrolateral orbital area (*VLO*) is mainly assessed upon differences in layers I, II, III and V. In the lateral orbital area layer II is dark, clustered and well distinguishable from layer III, while in the ventrolateral orbital area no clear distinction between layer II and layer III is visible, and layer II and III cells are arranged in curvilinear rows vertical to the pial surface. Generally, *VLO* is situated in the “notch” of the orbital surface of the frontal lobe. The “notch” is the dorsally directed indentation in the orbital cortical surface, which occurs in the middle of the line between the medial and the lateral side of the frontal lobe (see also Reep et al. 1996). In the notch, the layer I is wider but this is not a “sharp” feature to determine this boundary.

The border between *LO* and *VLO* is difficult to assess in the SMI 32-stained sections (Figs. 5b, 6a) as layers III, V and VI are stained in both the areas. However, the layers III, V and VI are well separated from each other in *LO* but generally not in *VLO*. In the parvalbumin stained sections (Fig. 6d), a lightly stained zone separates layer II–III from layer V in *LO*, whereas layers II, III and V are less heterogeneous in *VLO*, because of the darker background staining in *VLO*. In the calbindin-stained sections (Fig. 6b),

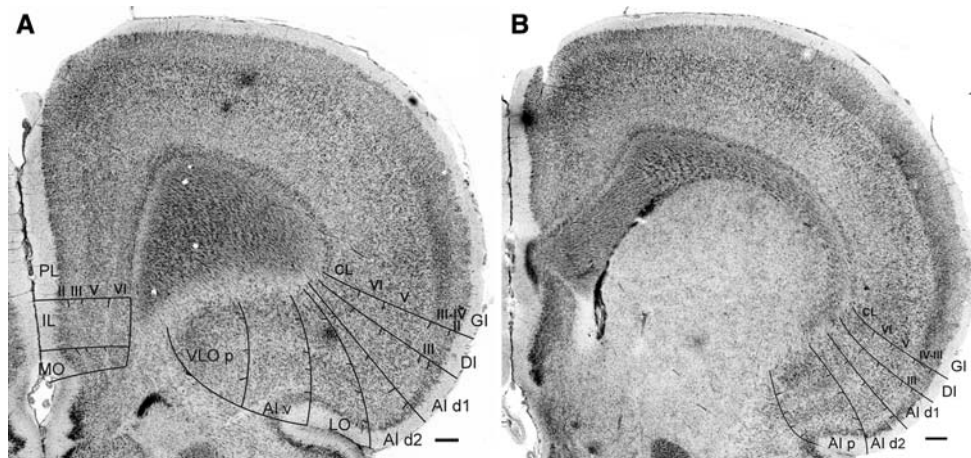


Fig. 8 In Nissl-stained sections, *GI* is distinguished by a densely packed, dark layer IV and a cell-sparse outer sublayer in layer V. The difference between *Al*_{d1} and *Al*_{d2} is especially visible in layers II and V. **a** In *IL*, layer II cells spread into layers I and III more than in *PL* and in *MO*. At the level of the Fig. 2 sixth panel, *LO* is wedged between *Al*_{d2} at its lateral and *Al*_v at its medial border. The large cells of layer V in *Al*_v are not arranged in vertical rows as they are in *Al*_d.

*VLO*_p can be distinguished by its more homogeneous appearance of the layers. The cells of the claustrum are dispersed in layer VI of *Al*_d and *LO*, but more densely packed underneath *Al*_v and *VLO*. **b** Section at same level as the eighth panel in Fig. 2. The characterizing feature of *Al*_p is the conspicuous separation of all (sub) layers and the claustrum. Scale bars 150 μm

layer II in *LO* is narrower than layer II in *VLO*. Moreover the calbindin-positive cells of layers II and III are arranged in vertical rows in *VLO*, but not so strongly in *LO*. The border between *LO* and *VLO* as seen in the calbindin-stained section (Fig. 6b) is in agreement with the border seen in the Nissl-stained sections. In the dopamine antibody staining (Fig. 6c), the border between *LO* and *VLO* is not distinguishable due to a lack of staining.

The difference between the ventrolateral orbital area (*VLO*) and its posterior part (*VLO*_p)

In Nissl-stained sections (Figs. 5a, 7, 10a), *VLO* is characterized by its layers II and III being homogeneous and their cells arranged in curvilinear rows, but with an open (i.e., low cell density) zone between layers III and V and/or layers V and VI. On the contrary, the most characteristic feature of the posterior part of *VLO* (i.e., *VLO*_p) is the homogeneity of all layers and the claustrum without so called open zones (Figs. 4a, 8a, 10b). The cells of the claustrum are larger than those in layer VI in *VLO*_p and thus we can distinguish the claustrum forming a sheath of cells beneath *VLO*_p.

The difference between *VLO* and *VLO*_p as described above for the Nissl-stained sections is also seen in SMI-32 stained sections (Figs. 5b, 4b) and in parvalbumin sections (Figs. 6d, 4d). In the calbindin and dopamine stained sections, no difference is visible between *VLO* and *VLO*_p due to an absence of staining in these areas (Figs. 6b, c, 4c, e).

The ventrolateral orbital, posterior part (*VLO*_p) and the ventral agranular insular (*Al*_v) area

The area *Al*_v borders medially *VLO*_p. In the Nissl-stained coronal sections the different layers are well visible in *Al*_v, whereas they are not in *VLO*_p (Fig. 4a).

In the SMI-32 staining (Fig. 4b), the layers are more visible in *Al*_v than in *VLO*_p. The layers in *VLO*_p show a more homogeneous staining. In the parvalbumin antibody staining (Fig. 4d), *VLO*_p is homogeneously stained, while in *Al*_v layer V is very prominent (Fig. 4d). In the calbindin staining (Fig. 4e), the border between *Al*_v and *VLO*_p is assessed by extrapolation from the border in the Nissl staining. In *Al*_v, layer II has a sharper border on layer III than in *VLO*_p (Fig. 4e). The dopamine antibody stained section does not show a sufficient difference between *Al*_v and *VLO*_p due to an absence of staining in these areas. Therefore, the border between these areas in Fig. 4c is extrapolated from Nissl and other stainings.

The ventrolateral orbital (*VLO*) and the ventral orbital (*VO*) area

In Nissl-stained sections (Figs. 6e, 7), layer III in *VO* is less densely packed than layer III in *VLO*. In layers II and III in *VLO*, the somata are arranged in vertical rows, but this feature is much less or absent in *VO* (Fig. 7a). *VO* is the most rostral area of the orbital cortex to connect the frontal lobe with the retrobulbar region (Fig. 10a).

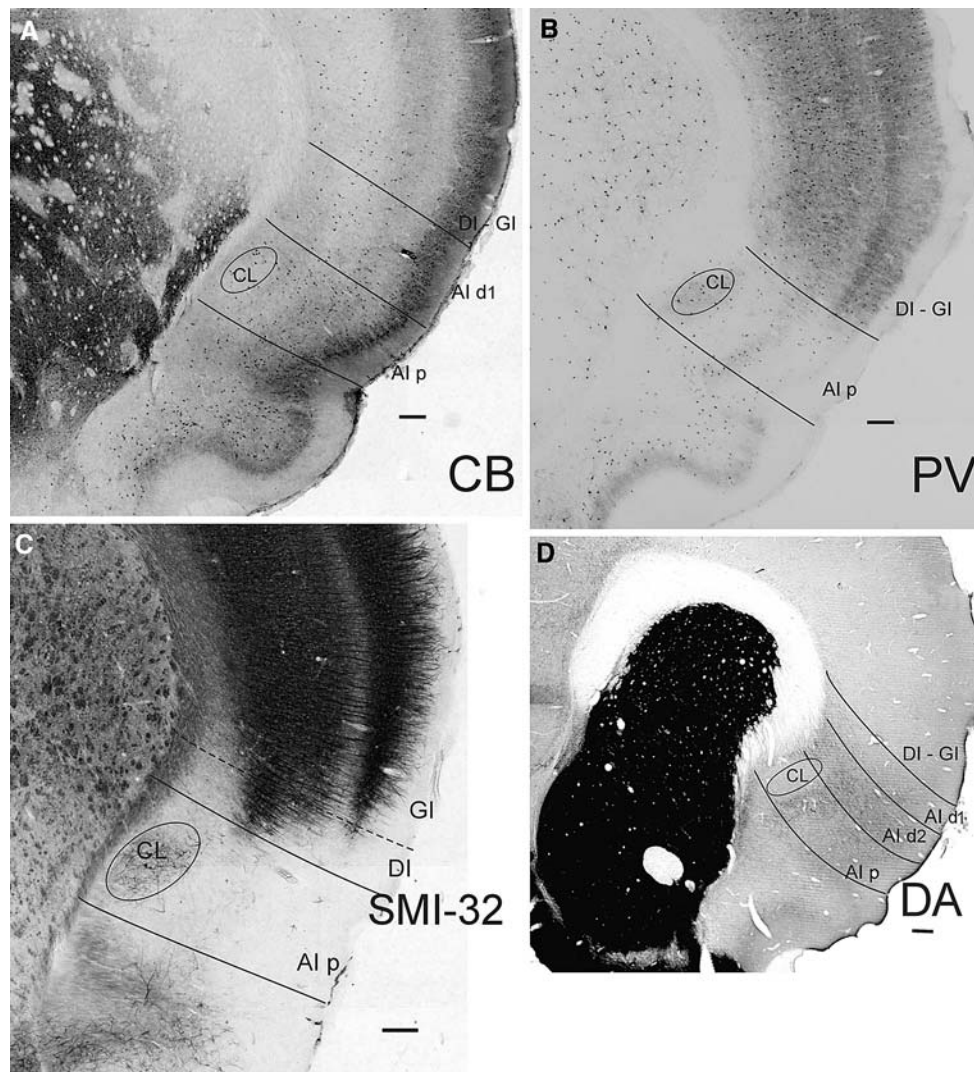


Fig. 9 **a** In *Alp*, layer V contains more calbindin-positive cells than in *Ald₂* (see Fig. 4e). The dorsal border of *Ald₁* is drawn by extrapolation from a nearest consecutive Nissl staining; caudal to level of eighth panel in Fig. 2. **b** Only a few PV-positive cells are stained in *Alp*, whereas parvalbumin staining in the dysgranular and granular insular cortex is more abundant. The claustrum (*CL*) is visible as a small area with some higher concentration of large PV-

positive cells. **c** *Alp* shows a lack of SMI-32 staining with exception of a large part of the claustrum. **d** DA staining, section at ~ level rostral to panel eight in Fig. 2. In *Alp*, less dopaminergic fibers are visible than in *Ald₂*, especially in the more superficial layers. The oval region without dopamine staining lies in the claustrum (*CL*). Scale bars 150 μ m

In the SMI-stained sections (Figs. 5b, 6a), the staining in layers III, V and VI is prominent in VLO, but in VO staining of layer III is absent and staining of layers V and VI is clearly less than in VLO. In general, the SMI-32 staining of layers is more prominent in VLO than in VO. The calbindin-stained sections are comparable to the Nissl-stained sections with VLO showing a columnar structure in layers II and III, which is not well visible in VO (Fig. 6b). In the parvalbumin-stained sections (Fig. 6d), the layers II and III are generally less densely packed and smaller in VO than in VLO and layer V is narrower in VO than in VLO. In the dopamine-stained section (Fig. 6c), no conspicuous distinction between VLO and VO is found due to a lack of staining.

The ventral orbital (VO) and the medial orbital (MO) area

In Nissl-stained sections (Figs. 5a, 6e, 7), the border between the ventral orbital area (VO) and the medial orbital area (MO) is found near the ventro-medial crown of the frontal lobe. In MO, layer II has a sharp border upon layer III, while in VO the layers II and III have a vague border as their cells mix. The cells in layer II in MO are also more equally distributed than in layer II in VO. In general, layer III in MO is less densely packed than layer III in VO. This gives the impression that layer II lies as a sheath/rim over layer III in MO, whereas this is not the

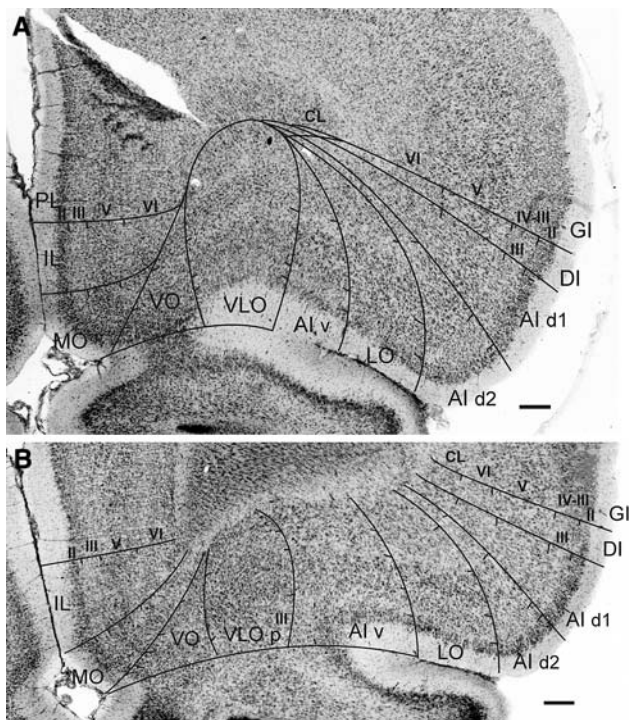


Fig. 10 In *VLO*, the differences between the Nissl stained layers are better visible than in *VLOp*, cf. **a** at the level between the fourth and fifth panel in Fig. 2. **b** Nissl-stained section showing difference between *LO* and *Alv*. Scale bars 150 μ m

case in *VO*. The cells in layer V in *MO* are also arranged in closely lying vertical rows, which is not the case in the *VO*.

In the SMI-32 stained sections (Figs. 5b, 6a), no difference is found between *MO* and *VO*. At the other hand, dopamine staining shows much more fibers in *MO* than in *VO* in Fig. 6c. In *VO*, however, many intensely stained fibers are visible, when *VO* is connected with the retrobulbar region (Fig. 4c) due to dopaminergic fibers passing through the retrobulbar area and the PFC. In the calbindin-stained sections (Fig. 6b), the layer II is well stained in *VO*, but in general less in *MO* where cells are more dispersed in layer II. This clear border between *VO* and *MO* found in the calbindin-stained sections is in agreement with the border in the Nissl-stained sections. The difference between *VO* and *MO* is also present in the parvalbumin-stained sections as the cells of layer II in *MO* are much less densely packed than those in layer II in *VO*. In addition, layer V in *MO* is broader, though less stained than layer V in *VO* (Fig. 6d).

The medial orbital (*MO*) and the infralimbic (*IL*) area

In Nissl-stained sections (Figs. 4a, 8a, 10), the layers II, III and V in the infralimbic area (*IL*) tend to be rather homogeneous, especially the layers III and V. Some

difference, however, may still be seen between layer II and III in *IL*. As a rule, the various layers in *MO* are well distinguishable from each other. An important difference between both the areas is generally found in layer II cells. In *IL*, they spread diffusely into layer I as well as into layer III, while in *MO*, layer II has a sharper border upon layers I and III (Figs. 4a, 10).

In the dopamine-antibody staining, *MO* and *IL* are not distinguishable from each other (Fig. 4c). This is also true for the SMI-32 staining (Figs. 4b, 5b). In the calbindin staining (Fig. 4e), *IL* is distinguished by a broad layer II, extending into layers I and III, whereas the CB staining in layer II of *MO* is “narrow” and less.

In the parvalbumin staining, layer II is in general less stained in *IL* than in *MO*.

The medial orbital (*MO*) and the prelimbic (*PL*) area

In the anterior part of the frontal lobe, *MO* borders dorsally not with *IL*, but with *PL* (Figs. 1, 2). In Nissl-stained sections (Fig. 7), the border between *MO* and the prelimbic area (*PL*) is characterized by layer III. This layer is visible in *PL* as a light band that contrasts with the dark layers II and V. This light band ends at the border on *MO*. Therefore, the contrast between layers II, III and V is much less in *MO* and *IL* than in *PL*. The layer II in *MO* is thicker than in *PL*. In layer V, the cells are arranged in rows in *MO*, but not in *PL*. The cells in layer V are smaller and more densely packed in *MO* than in *PL*.

There is no significant change between *MO* and *PL* in the SMI-32 staining (Fig. 6a). The border is very clear in the calbindin-stained sections (Fig. 6b) as layer II is densely stained in *PL*, but less in *MO*. In the parvalbumin-stained sections, some background staining is seen in *MO*, but not in *PL* (Fig. 6d). The dopamine-stained fibers are denser in *PL* than in *MO* (Fig. 6c). In the dopamine antibody stained sections, layers III–V in *PL* are in general more stained than in *MO* (Fig. 6c).

Discussion

This paper provides the cytoarchitectonic criteria to determine the boundaries of the orbital and agranular insular areas in such a detail, that they can be located at the same position by independent anatomists. This is a prerequisite for stereological studies, since for studying e.g. total number of neurons it is a necessary condition to determine the borders of areas of interest (Rajkowska et al. 2005; Uylings et al. 2005; Markram et al. 2007). These cytoarchitectonic criteria are observed in the Nissl-stained sections of all rat brains examined. Each cytoarchitectonic-

defined boundary is corroborated by one or more immunocytochemical stainings applied. Each immunocytochemical staining, however, shows a characteristic subset of the cytoarchitectonical borders. This is shown in the summary Table 1.

These cytoarchitectonic and chemoarchitectonic areas comply in large lines with those described by Ray and Price (1992) and Reep et al. (1996), who relied mainly upon thalamic connections; with the exception of the rostral part and the new subareas detected. The new findings are (a) the distinction of the new subarea VLOp, i.e., the posterior part of the ventrolateral orbital area, (b) a further subdivision of AId and DLO into a dorsal and ventral part: AId₁ and AId₂, and DLO₁ and DLO₂, respectively, (c) the rostral extension of the orbital areas, and (d) AIv bordering laterally also with LO in the rostral part of AIv. The cytoarchitectonic division of AId and DLO in a dorsal and ventral part is supported by the marked difference in density of dopaminergic fibers and also by the differences visible in the calbindin staining. In mouse, this cytoarchitectonic difference between dorsal and ventral part is more prominent (Van de Werd, Rajkowska, Evers and Uylings, in prep.). In the coronal sections of the rostral pole, not all cortical layers are visible. Still sufficient cytoarchitectonic and chemoarchitectonic features of orbital subareas remain noticeable, which allow us to follow the boundaries until their ending in the rostral pole. In this respect we differ from Ray and Price (1992), who distinguished a separate medial and lateral frontal polar area (FPm and FPl) in this rostral part of the prefrontal cortex. As a result, the orbital subareas defined in this paper extend into the rostral pole and no FPm and FPl have been specified. Like Ray and

Price (1992), we recognize the dorsolateral area (DLO) and the dorsal agranular insular area (AId) in the lateral prefrontal cortex. These differences are seen in a transitional zone. Therefore, the transition of DLO into AId is related to the presence of claustrum underneath AId. Groenewegen (1988), Uylings and Van Eden (1990) and Uylings et al. (2003) did not include the posterior agranular insular area (AIp) and the dysgranular insular area (DI) in the PFC. This was based upon the connectivity with the mediodorsal nucleus and the midline and intralaminar nuclei of the thalamus (Groenewegen and Berendse 1994). DI is identified by us as a smaller area than the one described by Cechetto and Saper (1987) and Saper (2004), but is in agreement with the size and location of the DI reported by Ray and Price (1992).

Figures of sections stained with SMI-32, parvalbumin and calbindin antibodies are also found in Paxinos et al. 1999. These images in Paxinos et al (1999) agree largely with our results taking into account their darker staining. In a few aspects they differ: We have a larger contrast between DLO, AId 1 + 2 and AIp and their neighboring areas of the PFC, and in VLO in the SMI-32 staining. In our calbindin staining, the differences between DLO₁ and DLO₂, and AId₁ and AId₂ are easier to distinguish. The results of our DA staining are compatible with the results obtained with the tyrosine hydroxylase (TH) staining in Paxinos et al. (1999).

Behavioral studies indicate, that the orbital PFC is involved in supporting reversal learning in both primates and rats (McAlonan and Brown 2003; Chudusama and Robbins 2003; Murray et al. 2007). The medial PFC is involved in supporting rule switching and attentional set shifting in rats (De Bruin et al. 1994; Ragozzino 2007; Van der Plasse et al. 2007) and is implicated in instrumental learning (Fuyashiki and Gallagher 2007) more than the orbital PFC. The orbital PFC is reported to be important for updating stimulus-outcome in Pavlovian associations (Ostlund and Balleine 2007). These behavioral studies rely on electrochemical or chemical lesions of restricted areas in PFC. Electrophysiological studies of Roesch et al. (2006) reveal that neurons, recorded mainly in the LO subarea, code especially for temporal features of reward and not for the spatial features of reward. Feierstein et al. (2006), on the other hand, show that a relatively large proportion of neurons code for spatial features of reward. They recorded neurons mainly in the VLO area. These two studies indicate, that orbital PFC is not a functionally homogeneous area (Zald, 2006). Furthermore, we can assume, that each of the cytoarchitectonically different subareas does differ in several aspects in their connectivity circuitries (Uylings et al. 2003; Jones et al. 2005). Therefore, we can predict, that behavioral and electrophysiological studies distinguishing different orbital

Table 1 Comparison of detectable borders in different stainings

Borders	Nissl	SMI-32	DA	PV	CB
G/DLO ₁	+	+	–	±	±
DLO ₁ /DLO ₂	+	–	++	±	+
DLO ₂ /LO	++	+	++	+	+
LO/VLO	++	±	±	±	+
VLO/VO	+	±	+	±	+
VO/MO	+	–	+	+	++
MO/IL	++	–	–	–	–
MO/PL	+	–	±	+	++
DI/AId ₁	++	+	–	+	±
AId ₁ /AId ₂	+	–	++	±	+
AId ₂ /AIv	++	+	++	+	+
AIv/LO	+	±	–	±	–
AIv/VLOp	++	+	±	+	±
VLO/VLOp	++	++	–	+	+

++ clearly definable; + definable; ± difficult definable; – not definable

subareas specified in this paper will forward our understanding of the functional networks in the orbital and insular PFC.

The cytoarchitectonic defined orbital and agranular insular areas can be used also as a template for the description of tracing studies (Gabbott et al. 2005; Hoover and Vertes 2007; Groenewegen et al. 2007). This is more important, since an open question still exists whether or not the whole orbital cortex belongs to the PFC, especially the VLO has been questioned (Reep et al. 1996; Uylings et al. 2003; Groenewegen et al. 2007). At this moment some similarities have been pointed out between primate and rat orbital cortex (Murray et al. 2007), but also some differences (Furuyashiki and Gallagher 2007). Future tracing studies will enable a more appropriate comparison between networks of primate and rodent orbital cortex areas.

Acknowledgments We acknowledge the expert histological assistance of Ing. P. Evers (Neth. Brain Bank, Amsterdam).

References

- Cechetto DF, Saper CB (1987) Evidence for a viscerotopic sensory representation in the cortex and thalamus in the rat. *J Comp Neurol* 262:27–45
- Chudasama Y, Robbins TW (2003) Dissociable contributions of the orbitofrontal and infralimbic cortex to pavlovian autoshaping and discrimination reversal learning: further evidence for the functional heterogeneity of the rodent frontal cortex. *J Neurosci* 23:8771–8780
- De Brabander JM, van Eden CG, de Bruin JPC, Feenstra MGH (1992) Activation of mesocortical dopaminergic system in the rat in response to neonatal medial prefrontal cortex lesions. Concurrency with functional sparing. *Brain Res* 581:1–9
- De Bruin JPC, Sanchez-Santed F, Heinsbroek RP, Donker A, Postmes P (1994) A behavioural analysis of rats with damage to the medial prefrontal cortex using the Morris water maze: evidence for behavioural flexibility, but not for impaired spatial navigation. *Brain Res* 652:323–333
- Feierstein CE, Quirk MC, Uchida N, Sosulsky DL, Mainen ZF (2006) Representation of spatial goals in rat orbitofrontal cortex. *Neuron* 51:495–507
- Furuyashiki T, Gallagher M (2007) Neural encoding in the orbitofrontal cortex related to goal-directed behavior. *Ann N Y Acad Sci* (Epub ahead of print 14 August)
- Gabbott PLA, Warner TA, Jays PRL, Salway P, Busby SJ (2005) Prefrontal cortex in the rat: projections to subcortical autonomic, motor and limbic centers. *J Comp Neurol* 492:145–177
- Geffard M, Buijs RM, Seguela P, Pool CW, Le Moal M (1984) First demonstration of highly specific and sensitive antibodies against dopamine. *Brain Res* 294:161–165
- Groenewegen HJ (1988) Organization of the afferent connections of the mediodorsal thalamic nucleus in the rat, related to the mediodorsal-prefrontal topography. *Neuroscience* 24:379–431
- Groenewegen HJ, Berendse HW (1994) The specificity of the ‘nonspecific’ midline and intralaminar thalamic nuclei. *Trends Neurosci* 17:52–57
- Groenewegen HJ, Witter MP (2004) Thalamus. In: Paxinos G (ed) *The rat nervous system*, 3rd edn. Academic Press/Elsevier, San Diego pp. 407–453
- Groenewegen HJ, Schilman E, van de Werd HJ, Galis-de Graaf Y, Joel D, Uylings HBM (2007) Organization of the projections of different orbitofrontal cortical areas to the striatum and thalamus in rats. Soc Neurosci Meeting, November 2007
- Hof PR, Morrison JH (1995) Neurofilament protein defines regional patterns of cortical organization in the macaque monkey visual system: a quantitative immunohistochemical analysis. *J Comp Neurol* 352:161–186
- Hoover WB, Vertes RP (2007) Anatomical analysis of afferent projections to the medial prefrontal cortex in the rat. *Brain Struct Funct* 212:149–179
- Jones BF, Groenewegen HJ, Witter MP (2005) Intrinsic connections of the cingulate cortex in the rat suggest the existence of multiple functionally segregated networks. *Neuroscience* 133:193–207
- Kalsbeek A, De Bruin JPC, Feenstra MGP, Uylings HBM (1990) Age-dependent effects of lesioning the mesocortical dopamine system upon prefrontal cortex morphometry and PFC-related behaviors. *Prog Brain Res* 85:257–282
- Kamstra AW, Uylings HBM (1983) A Teflon-disc for processing loose, serial celloidin sections. *Stain Technol* 58:231–232
- Krettek JE, Price JL (1977) The cortical projections of the mediodorsal nucleus and adjacent thalamic nuclei in the rat. *J Comp Neurol* 171:157–191
- Markham JA, Morris JR, Juraska JM (2007) Neuron number decreases in the rat ventral, but not dorsal and medial prefrontal cortex between adolescence and adulthood. *Neuroscience* 144:961–968
- McAlonan K, Brown VJ (2003) Orbital prefrontal cortex mediates reversal learning and not attentional set shifting in the rat. *Behav Brain Res* 146:97–103
- Murray EA, O’Doherty JP, Schoenbaum G (2007) What we know and do not know about the functions of the orbitofrontal cortex after 20 years of cross-species studies. *J Neurosci* 27:8166–8169
- Ostlund SB, Balleine BW (2007) Orbitofrontal cortex mediates outcome encoding in Pavlovian but not instrumental conditioning. *J Neurosci* 27:4819–4825
- Paxinos G, Kus L, Ashwell KWS, Watson C (1999) *Chemoarchitectonic atlas of the rat forebrain*. Academic Press, San Diego
- Ragozzino M (2007) The contribution of the medial prefrontal cortex, orbitofrontal cortex and dorsomedial striatum to behavioral flexibility. *Ann N Y Acad Sci* (Epub ahead of print 14 August)
- Rajkowska G, Miguel-Hidalgo JJ, Dubey P, Stockmeier CA, Krishnan KR (2005) Prominent reduction in pyramidal neurons density in the orbitofrontal cortex of elderly depressed patients. *Biol Psychiatry* 58:297–306
- Ray JP, Price JL (1992) The organization of the thalamocortical connections of the mediodorsal thalamic nucleus in the rat, related to the ventral forebrain-prefrontal cortex topography. *J Comp Neurol* 323:167–197
- Reep RL, Corwin JV, King V (1996) Neuronal connections of orbital cortex in rats: topography of cortical and thalamic afferents. *Exp Brain Res* 111:215–232
- Roesch MR, Taylor AR, Schoenbaum G (2006) Encoding of time-discounted rewards in orbitofrontal cortex is independent of value representation. *Neuron* 51:509–520
- Saper CB (2004) Central autonomic system. In: Paxinos G (ed) *The rat nervous system*, 3rd edn, Academic Press/Elsevier, San Diego, pp. 761–796
- Uylings HBM, Groenewegen HJ, Kolb B (2003) Do rats have a prefrontal cortex? *Behav Brain Res* 146:3–17
- Uylings HBM, Van Eden CG (1990) Qualitative and quantitative comparison of the prefrontal cortex in rat and primates, including humans. *Prog Brain Res* 85:31–62
- Uylings HBM, Malofeeva LI, Bogolepova IN, Jacobsen AM, Amunts K, Zilles K (2005) No postnatal doubling of number of neurons

- in human Broca's area (BA 44 and 45)? A stereological study. *Neuroscience* 136:715–728
- Van der Plasse G, La Fors SSBM, Meerkerk DTJ, Joosten RNJMA, Uylings HBM, Feenstra MGP (2007) Medial prefrontal serotonin in the rat is involved in goal-directed behaviour when affect guides decision making. *Psychopharmacology* (Epub ahead of print August)
- Van Eden CG, Uylings HBM (1985) Cytoarchitectonic development of the prefrontal cortex in the rat. *J Comp Neurol* 241:253–267
- Zald DH (2006) The rodent orbitofrontal cortex gets time and direction. *Neuron* 51:395–397